Available online at www.sciencedirect.com

SCIENCE DIRECT®

Biochimica et Biophysica Acta 1665 (2004) 156–166

BIOCHIMICA ET BIOPHYSICA ACTA
BBA

http://www.elsevier.com/locate/bba

The effect of bacteriorhodopsin, detergent and hydration on the cubic-to-lamellar phase transition in the monoolein–distearoyl phosphatidyl glycerol–water system

Emma Sparr[a,*], Pia Wadsten[b], Vitaly Kocherbitov[c], Sven Engström[b]

[a]*Department of Pharmacy, Uppsala University, Box 580, SE-751 23 Uppsala, Sweden*
[b]*Materials and Surface Chemistry, Chalmers University of Technology, SE-412 96 Göteborg, Sweden*
[c]*Department of Physical Chemistry 1, Center for Chemistry and Chemical Engineering, Lund University, Lund, Sweden*

Received 12 June 2003; received in revised form 13 July 2004; accepted 27 July 2004
Available online 17 August 2004

Abstract

The cubic phase of monoolein (MO) has successfully been used for crystallization of membrane proteins. It is likely that the transition to a lamellar phase upon dehydration is important for the crystallization process, and that the internal dimensions of the lipid phases (i.e., water pore diameter) are crucial for the inclusion and the diffusion of membrane proteins. In the present study, we investigated the cubic-to-lamellar phase transitions in the MO–water and the MO–distearoyl phosphatidyl glycerol (DSPG) systems. The MO–water system was investigated by means of isothermal sorption and desorption microcalorimetry. We show that the transition from cubic to lamellar phase induced by desorption is driven by entropy. At 25 °C, this occurs at a water activity of 0.98 with a transition enthalpy of 860 J/mol (MO). The phase behavior was also investigated in the presence of a small amount of the transmembrane protein bacteriorhodopsin (bR), and a detergent, octyl glucoside (OG), and it was shown that both bR and OG stabilize the lamellar phase. Analogous results were obtained for the MO–DSPG–water system. The latter system resembles the MO–water system in that a cubic-to-lamellar phase transition is induced by dehydration, although the structural properties of these phases are slightly different. Finally, we demonstrate that bR can be crystallized from a cubic phase of MO–DSPG-buffer.

Keywords: Protein crystallization; Lipid phase transitions; Isothermal microcalorimetry; Small angle X-ray scattering (SAXS); Monoolein (MO); Distearoyl phosphatidyl glycerol (DSPG)

1. Introduction

In 1996, Landau and Rosenbusch [1] demonstrated that cubic phases formed of monoolein (MO) and water could be used for crystallization ('in cubo') of membrane proteins. This discovery opened a new field in protein crystallography, and it raised a broader interest for the MO liquid crystalline phases. However, to our knowledge only six membrane proteins have been crystallized in cubo [1–6]. One reason for the success of the MO cubic phase in protein crystallization may lie in the anomalous phase behavior of MO and water upon dehydration. The low output, on the other hand, may be due to the geometrical limitations of the cubic phase, i.e., the relatively narrow water channels. A deeper understanding of the physical and chemical properties of the MO–water system with and without proteins and crystallization agents is therefore desirable in order to extend its applicability for protein crystallization.

The phase diagram of MO and water shows remarkable features, indicating specific intermolecular interactions [7,8]. In excess water, a reversed cubic liquid crystalline phase, belonging to space group $Pn3m$, is present, which is

* Corresponding author. Present address: Department of Physical Chemistry 1, Center for Chemistry and Chemical Engineering, Lund University, Lund, Sweden. Tel.: +46 46 222 48 12; fax: +46 46 222 44 13.
E-mail address: emma.sparr@fkem1.lu.se. (E. Sparr).

0005-2736/$ - see front matter © 2004 Elsevier B.V. All rights reserved.
doi:10.1016/j.bbamem.2004.07.005

transformed to another cubic phase, belonging to space group *Ia*3*d*, upon dehydration [8]. The structure of the cubic phases is modeled as infinite periodic minimal surfaces (IPMS) in which the mid-plane of the MO bilayer forms the IPMS and the bilayer is surrounded by two separate water channel systems. The cubic phase at the higher water contents forms an IPMS of the diamond type (C_D), and the cubic phase at lower water contents is of the gyroid type (C_G). The bicontinuity of the cubic phases allows for diffusion in three dimensions in both the lipid and water regions.

The cubic phases can be transformed to a lamellar liquid crystalline phase (L_α) upon further dehydration. The transition from a bicontinuous C_G cubic phase, having a slightly negative curvature in the plane of the polar headgroups (i.e., the bilayer tends to circumvent water), to a lamellar phase of planar bilayers (i.e., with zero curvature) is not expected on grounds of the curvature arguments, and makes the MO–water systems anomalous in this respect. Most lipid/surfactant–water systems form self-assembly structures of decreasing curvature (i.e., more negative) as the water content decreases [9]. In a crystallization setup, the addition of salt and/or polymer to the lipid–protein cubic phase is expected to dehydrate the sample, and possibly induce a lamellar phase [10]. It is therefore plausible that the anomalous MO lamellar-to-cubic phase transition has a crucial role in the in cubo crystallization process.

Most trans-membrane proteins have a close to cylindrical shape, and one can expect better hydrophobic match between the proteins and the planar bilayer of the lamellar phase than between the proteins and the curved (although saddle-point like) bilayer of the cubic phases [10]. It was postulated that the proteins partition into the lamellar phase and, in addition, that proteins may induce domains of planar bilayers within the cubic phase. This hypothesis is supported by examination of lipid–protein samples after crystal growth, which has shown a lipid cubic phase with patches of lamellar sheets surrounding protein crystals [10]. It is also very likely that the internal dimensions of the cubic and the lamellar phases are crucial for reconstitution and diffusion of membrane proteins. The dimensions of the aqueous regions in the cubic phase can be regulated by the chemical composition, for example by the addition of distearoyl phosphatidyl glycerol, DSPG, an anionic lipid present in bacterial membranes. Engblom et al. [11] have previously investigated the phase behavior of the ternary MO–DSPG–water system at room temperature. Besides the C_G and the C_D cubic phases, a primitive C_P (body-centered space-group, *Im*3*m*) cubic phase is formed in the MO–DSPG–water system. The latter cubic phase can take substantially more water (about 70% w/w) than the *Pn*3*m* cubic phase formed in the binary MO–water system (about 40% w/w). Similar to the MO–water system, the cubic phases of MO–DSPG–water are transformed into a lamellar phase upon dehydration [11]. DSPG alone forms a lamellar phase in water above its chain-melting temperature [12].

In this work, we investigate the cubic-to-lamellar phase transition of the MO–water system in some detail by means of sorption/desorption calorimetry, and we study the effects caused by the membrane protein bacteriorhodpsin (bR) and/or a detergent often present in crystallization experiments, β-octyl glycopyranoside (OG). From the calorimetry results, we conclude that the spontaneous lamellar-to-cubic transition is entropically driven. Moreover, it is demonstrated with partial phase diagrams that both bR and OG stabilize the lamellar phase at low water contents in the MO–water and MO–DSPG–water systems. Finally, we demonstrate that bR can be crystallized from a DSPG/MO cubic phase.

2. Materials and methods

2.1. Materials

1-Monooleoyl-*rac*-glycerol was purchased from Sigma (St. Louis, MO), 99% purity (used in microcalorimetry and crystallization experiments), and Danisco Cultor A/S (Brabrand, Denmark), 94.9% (used in phase studies). The phase behavior of the purified and the technical MO–water mixtures are qualitatively similar, although the positions of the phase transitions are slightly different [7,8,13].

The sodium salt of DSPG was purchased from Genzyme Pharmaceuticals (Liestal, Switzerland) and *n*-octyl β-D-glycopyranoside was purchased from Anatrace (Maumee, OH). Bacteriorhodopsin from *Halobacterium halobium* was purchased from Sigma (lyophilized powder, minimum 75% bR).

2.2. Sorption (and desorption) calorimetry

MO was dried in vacuum in contact with molecular sieves during 24 h before use. For sorption experiments, it was placed into the calorimetric cell in a glove bag filled with dry nitrogen. For the desorption experiments, the required composition of lipid–water mixture was prepared directly in the calorimetric cell. Sorption measurements were conducted using a sorption calorimeter [14,15]. The sorption calorimetric cell consists of two chambers: the sorption chamber, where the studied sample is placed, and the vaporization chamber, filled with liquid water. Water evaporates, and then diffuses through a tube to the sorption chamber where it is absorbed by the sample. The cell is placed into a double twin microcalorimeter [16], which separately measures thermal powers released in the two chambers. From the measured thermal powers, one can calculate the activity of water and the enthalpy of mixing of water as a function of the sample composition. Using the desorption method, one can obtain the same parameters as in the sorption method as well as enabling studies at very

high water activities. In the desorption calorimetric method, water evaporates from the water-rich sample, diffuses into the condensation chamber and is then condensed into a salt solution [17].

2.3. Phase studies

To be able to reconstitute bR in the lipid phase at low water contents, the samples had to be prepared in two steps. A suspension of bR in water was mixed with the dry lipid, and additional water was added to give a water concentration of approximately 40% w/w. The samples were centrifuged until the bR was uniformly distributed in the cubic phase, which was evidenced by the sample's homogeneous purple color. Dry lipid was then added to reach the desired concentration, and the samples were again centrifuged until bR was homogeneously distributed in the lipid phase. All samples were prepared so that the lipid/bR ratio was kept constant, while the water content was varied. The phase characterization was performed within 2 days after sample preparation, as the protein was less stable in samples of low water content compared to the more swollen cubic phase. Denaturation of the protein was clearly observed as bleaching of the samples. Uncolored samples were not further investigated. Phase characterization was performed by visual inspection and with Small Angle X-ray Scattering (SAXS). Anisotropy was detected using crossed polarizers.

2.3.1. SAXS

The measurements were carried out on a Kratky compact small angle system (HECUS MBraun, Graz, Austria) equipped with a position-sensitive detector, containing 1024 channels of 55-μm width. A monochromator with a nickel filter was used to select the Cu K_α radiation (λ=1.542 Å) provided by the generator. The sample to detector distance was 282 mm. The samples were prepared in a paste holder with thin mica windows. The temperature in the sample cell was regulated by a Peltier element (accuracy ±0.1 °C). The camera volume and the sample cell were held under vacuum to minimize the scatter from the air.

2.4. Protein crystallization

The lyophilized powder of bR was suspended in 25 mM Na/K-P_i, pH 6.9 and 1.2% w/v OG. The detergent to protein ratio used for solubilization was 20:1. Following sonication (1 min, 35 kHz), the solution was incubated in the dark for 24 h. The pH was then adjusted with 0.1 M HCl to 5.5 and centrifuged (45 min at 200,000×g). The supernatant was collected and concentrated. bR concentrations were determined spectrophotometrically at 550 nm (ε=5.8×10^4 M^{-1} cm^{-1}) [1]. To form a transparent cubic phase of the primitive (C_P) and the gyroid (C_G) types, DSPG was mixed with MO and buffer as described in Ref. [11]. Cubic phases were prepared by mixing MO with buffer containing DSPG, bR, salt and OG (1.2% w/v) to yield a final volume of 40 μl. This was followed by centrifugation [18]. Bicontinuous cubic phases of C_P and C_G contained 44–47% w/w MO, 49.5–51% w/w bR-solution and 2–5.5% w/w DSPG. Cubic phase of the diamond (C_D) type contained 60% w/w MO, no DSPG and 40% w/w bR-solution. Components were added in the following order: (i) MO, (ii) DSPG dispersed with bR stock solution, 18 mg/ml in 25 mM Na/K-Pi buffer, pH 5.6 with 1.5% OG to give a final protein concentration of 3.5 mg/ml, and (iii) 0.3 g Sørensen salt/g cubic phase [10]. The preparations were maintained in the dark at room temperature throughout crystallization.

3. Results and discussion

3.1. Sorption/desorption calorimetric studies of the MO–water system

The MO–water system was in investigated at temperatures between 25 and 50 °C by means of sorption and desorption calorimetry. For this we use a double twin sorption microcalorimeter that allows for simultaneous measurement of the partial molar enthalpy of mixing of water (ΔH_w) and the water chemical potential ($\Delta\mu_w$), expressed in terms of the osmotic pressure (Π_{osm}), or water activity (a_w) (Eq. (A3)). This method consequently provides a rather unique combination of thermodynamic information on of lipid hydration, including the partial molar enthalpy, the partial molar free energy and, thus also, the partial molar entropy of the hydration.

Fig. 1A shows the sorption data for the water activity as a function of water content for the lamellar and C_G cubic phases at 40 and 50 °C. The lamellar-to-cubic phase transition is observed as a tie line in the activity curves, where the length of the tie line corresponds to the amount of water taken up during the transition. In the beginning of the transition, the water activity has a small maximum, which indicates supersaturation of the lamellar phase with water before the formation of cubic phase. Such local maximum is typical for the transition to a cubic phase (see, for example, Ref. [19]). Subsequently, after the transition, the activity increases until the end of the experiment. The transition between the lamellar and cubic phases was not observed in sorption experiments at lower temperatures; therefore, desorption measurements were performed. The partial molar enthalpy curve from the desorption measurement at 25 °C is shown in Fig. 1B. The phase transition between the lamellar phase and the C_G cubic phase is observed as a peak in the enthalpy curve whereas a kink is observed in the activity curve (data not shown). Data from sorption and desorption measurements at different temperatures are summarized in Table 1. We conclude that the amount of water taken up during the transition, X_w(cub)–X_w(lam), increases with decreasing temperature. Furthermore, the transition occurs

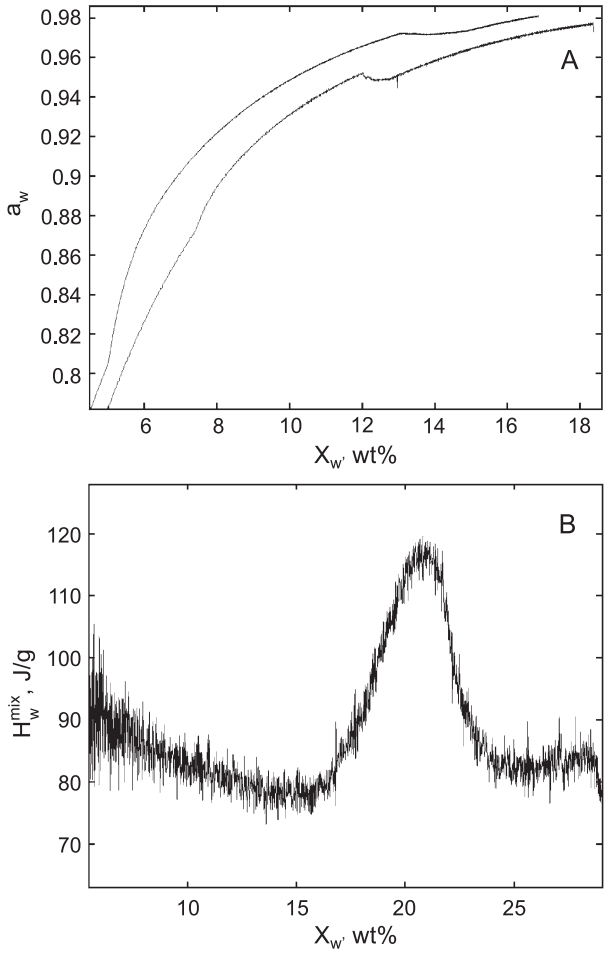

Fig. 1. Microcalorimetric sorption and desorption data. (A) Activity of water measured by sorption calorimetry in the composition range close to the transition from lamellar to cubic C_G phase at 40 °C (upper curve) and 50 °C (lower curve). (B) Partial enthalpy of mixing of water at 25 °C measured by desorption calorimetric technique.

at lower water contents/water activities when the temperature is increased.

From the calorimetric data, one can also obtain values of the transition enthalpy, $\Delta H^{L_\alpha \rightarrow C_G}$, and the transition entropy, $\Delta S^{L_\alpha \rightarrow C_G}$. By integrating the enthalpy curve over the phase transition (Fig. 1B, desorption data), we arrive at a transition enthalpy, $\Delta H^{L_\alpha \rightarrow C_G}$, of 860 J/mol (MO) at 25 °C, and from this we calculate the transition entropy, $\Delta S^{L_\alpha \rightarrow C_G}$, to 0.43 J/K/mol (per mole of mixture) (Eq. (A1)). In the sorption experiments, the enthalpy peak corresponding to the phase transition between the lamellar and the cubic phases could not be detected due to the high level of noise, which is typical for the measurements at high water activity. It was therefore not possible to calculate $\Delta H^{L_\alpha \rightarrow C_G}$. However, based on the temperature dependence in the activity curves (Fig. 1A), it was still possible to make a thermodynamic analysis of the phase transition using van der Waals differential equation (for details, see Appendix A). Based on this, the transition entropy was calculated from Eq. (A2) to 0.21 J/K/mol at 40 °C (Eq. (A2)). The difference in $\Delta S^{l \rightarrow 2}$ at different temperatures reflects the fact that the slope of the phase boundary becomes smaller at lower temperatures.

The calorimetric sorption measurement provides a relation between the water content and the osmotic pressure of water, $\Delta \Pi_{osm}$ (Eq. (A3)). The sorption data in Fig. 1A can therefore be directly interpreted as the repulsive interaction forces between the bilayers in the liquid crystalline phases.

The sorption data for the lamellar phase fit well to the exponential decaying repulsive force (Eq. (A4)). The decay lengths and the amplitudes at 25, 40 and 50 °C are summarized in Table 2. Experimental data of the repulsive interaction forces in the MO lamellar phase have, to our knowledge, not previously been reported. The values of spontaneous curvature, H_0, the rigidity bending constant, k_c, and the Gaussian curvature constant, k_g, in Table 2 are obtained from curve fitting the curvature elastic free energy (Eqs. (A5) and (A6)) to the experimental data of the free energy in the cubic phase. These values are in agreement with previously reported data for the same system obtained from osmotic stress measurements (H_0=8.01 · 10^{-3} Å at 35 °C) [20]. However, there is a significant disagreement with the spontaneous curvature reported by Vacklin et al. (H_0=2.5 · 10^{-2} Å at 37 °C) [21]. In the latter study, a long-chain hydrocarbon (e.g., tricosane) was added to the fully hydrated MO. Under these conditions, an inverse hexagonal H_{II} phase is formed at 37 °C rather than the inverse cubic phase that is formed in the MO–water system at the same temperature. The advantage of the method used by Vacklin et al. is that the packing frustration energy is lowered due to the presence of the hydrophobic alcohol, and the system exhibits a more homogeneous interfacial curvature [22]. However, as these data were obtained for a different system, no direct comparisons with H_0 obtained in the present study can be made.

As shown in Table 2, H_0 varies with temperature. It is also possible to alter H_0 by the addition of another lipid or detergent to the cubic phase, a situation relevant for in cubo crystallization. If the detergent promotes normal structures, e.g., the lamellar phase, H_0 will slightly increase, and vice versa. Variations in H_0 affect the curvature elastic free energy, which in turn will influence the phase behavior of the system. The integrated sorption data can be used to

Table 1
Properties of lamellar–cubic C_G phase transitions measured by sorption and desorption calorimetry

Temperature (°C)	X_w(lam)		X_w(cub)–X_w(lam)		a_w
	mol%	wt.%	mol%	wt.%	
50	72.2	11.6	2.0	1.1	0.948
40	74.7	13.0	2.3	1.5	0.972
25	80	17	5	6	0.98

X_w(lam) denotes the water content of the lamellar phase just prior to the phase transition, X_w (cub)–X_w (lam) is the water uptake during the transition and a_w is the water activity at the transition. Composition of phases X_w is given in molar and wt.% of water.

Table 2
Characteristics of the lamellar and cubic phases at T=25, 40 and 50 °C

Temperature (°C)	Lamellar phase		Cubic phase		
	F_0 ($\times 10^6$ N/m^2)	λ (Å)	H_0 ($\times 10^{-3}$ Å^{-1})	k_c ($\times 10^{-20}$ J)	k_g ($\times 10^{-22}$ J)
50	77.8	1.2	8.5	2.0	6.5
40	51.6	1.1	8.0	2.9	6.6
25	42.7	1.2	–	–	–

The constants are obtained by fitting of the experimental data to Eq. (A4) (lamellar phase) and Eqs. (A5) and (A6) (C_G cubic phase).

construct the free energy-composition phase diagram for the lamellar and cubic phases. Fig. 2 shows the energy curves calculated from the experimental data (Table 2), and for different values of H_0 (T=40 °C) (for details, see Appendix B). The figure shows that the phase transition between the lamellar and the cubic phases will occur at higher water contents when H_0 is increased.

3.2. Phase transition between lamellar and cubic phases in the MO–water system

The MO–water system was investigated at different temperatures. From the experimental data at 25 °C (Table 1), it is concluded that the transition between the cubic and the lamellar phases takes place at a_w=0.98, which corresponds to an osmotic pressure of 2.8 MN/m^2. Furthermore, the measured enthalpy for phase transition induced by dehydration is small (860 J/mol (MO)). This implies that the energy required to induce the lamellar phase is relatively low. The transition between the lamellar and the C_G cubic phase mainly involves a change in bilayer curvature, while the surface continuity is preserved. The resemblance between these phases results in a very small enthalpy change during the transition [23]. This has also been confirmed by differential scanning calorimetry (DSC) measurements, where the temperature-induced L_α–C_G transition at 50 °C (X_w=14.5 wt.%) was measured to 170 J/mol (MO) [24]. Phase transitions in sorption and DSC experiments are caused by changes of different parameters (water content and temperature, respectively), and can therefore not be directly compared without additional data. Nevertheless, the fact that both transition enthalpies are small confirms that the phases are energetically similar.

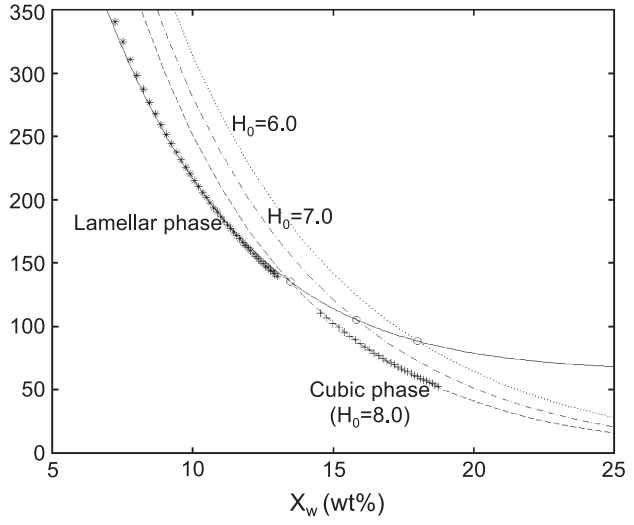

Fig. 2. Free energy composition diagram lamellar and cubic phases. The free energy obtained from the experimental data for the MO lamellar (*) and MO cubic phases (+) at T=40 °C, and the free energy profiles obtained by curve fitting of the experimental data to Eq. (A4) and Eqs. (A5) and (A6), respectively; (—) lamellar phase and (- - - -) cubic phase (H_0=8.0 Å^{-1}). The diagram can be used to predict the phase sequence, and the composition at the transition. Calculated profiles of the free energy for some different values of H_0 are also shown; H_0=7.0 Å^{-1} (-·-·-) and H_0=6.0 Å^{-1} (·····). The figure shows that the position of the phase transition between the lamellar and the cubic phases will occur at higher water contents when H_0 is increasing.

The combined thermodynamic data from the sorption and desorption measurements can be used to understand the swelling of the lamellar and cubic phases. The negative value of the free energy reflects the fact that these systems swell spontaneously when exposed to pure water. The hydration of the lamellar and cubic phases is accompanied by a small, close to uncertainty level, positive value of the partial molar enthalpy (about 1–2 kJ/mol of water) in all sorption and desorption experiments. Primarily, this demonstrates that the free energy and the partial molar enthalpy have opposite signs in the lamellar and cubic liquid crystalline phases, thus implying a positive value of the partial molar entropy. Therefore, the uptake of water in these phases must be favored by entropic effects. Furthermore, our study demonstrates that the transition between the cubic and the lamellar phases is not energetically favorable, as the enthalpy change of the transition is positive (Fig. 1B), and that the entropy change $\Delta S^{L_\alpha \rightarrow C_G}$ is positive. In other words, the phase transition is driven by entropy, which is an unusual property for phase transitions between different liquid crystalline phases. The transition from a reversed cubic phase to a lamellar phase upon dehydration cannot be explained using curvature arguments, as the transition from planar structure to structure with negative curvature is not expected upon addition of water. The increase of entropy is probably associated with changes occurring in lipid acyl-chains at different bilayer curvature.

3.3. Effects of OG and bR on the cubic-to-lamellar phase transition

We have investigated the equilibrium between the lamellar and cubic phases in mixtures of MO, DSPG, water

and small amounts of bR and/or OG. The results of the partial phase diagrams are shown in Figs. 3 and 4. For comparison, the phase boundaries obtained for the OG- and bR-free systems are also included in the figures (solid lines). The ternary and quaternary samples were prepared so that the ratios of OG/MO and bR/MO are kept constant to 1 and 0.5 wt.%, respectively, with the water content expressed as $X_w=m_w/m_{tot}$, where m_w is the amount of water and m_{tot} is the total mass of the sample.

Fig. 3 reveals that a transition from a cubic phase (C_G) to a lamellar phase in the MO–water system (solid lines) is induced either by a decrease in water content or temperature. The phase boundaries are in good agreement with previous data [13]. From Fig. 3 it is also evident that both OG and bR affect the phase behavior in favor of the lamellar phase. The strongest effect is observed when both detergent and protein are present (Fig. 3C).

The influence of bR and OG on the C_G-to-L_α phase transition was also investigated for the MO–DSPG–water system, lipid molar ratio 48.9:1 (lipid weight ratio 22.4:1). The samples were prepared so that the ratios of OG/(MO+DSPG) and bR/(MO+DSPG) were kept constant to 1 and 0.5 wt.%, respectively. The lipid composition was chosen to correspond to the C_P cubic phase at 50 wt.% water, which was the composition used in the crystallization setup. When this sample is dehydrated the C_G cubic phase is induced, followed by the lamellar phase [11]. The solid lines in the partial T–X_w phase diagrams in Fig. 4 correspond to the phase boundaries between the cubic (C_G) phase and the lamellar phase.

Analogous to the MO–water system, the phase transition from a cubic to a lamellar phase is induced by decreasing either the temperature or the water content. In the presence of OG or bR, the positions of the phase boundaries are translated towards higher temperatures and higher water contents (Fig. 4).

In order to explain the results caused by OG in Figs. 3A and 4A, the packing parameter concept of amphiphilic molecules can be used [25]. The basic idea is that the interfacial curvature of the bilayer increases or decreases depending on the molecular shape of the incorporated molecule. OG has a relatively large hydrophilic group, and is thus expected to promote normal (i.e., with positive (circumventing oil) curvature) structures. This effect is revealed as a stabilization of the lamellar phase. The phase boundaries in Fig. 3A are shifted by approximately 2 °C, which implies a strong effect counted per OG molecule. In a theoretical description of the phase equilibrium between the cubic and the lamellar phases, the addition of a small amount of a lamellar-forming detergent to the MO cubic phase can be represented by a change in the spontaneous curvature, H_0. When H_0 comes closer to zero, i.e., when the bilayer becomes closer to planar, the phase transition will occur at higher water contents. The results in Fig. 2 can therefore be directly related to the translation of the phase boundaries in Fig. 3A.

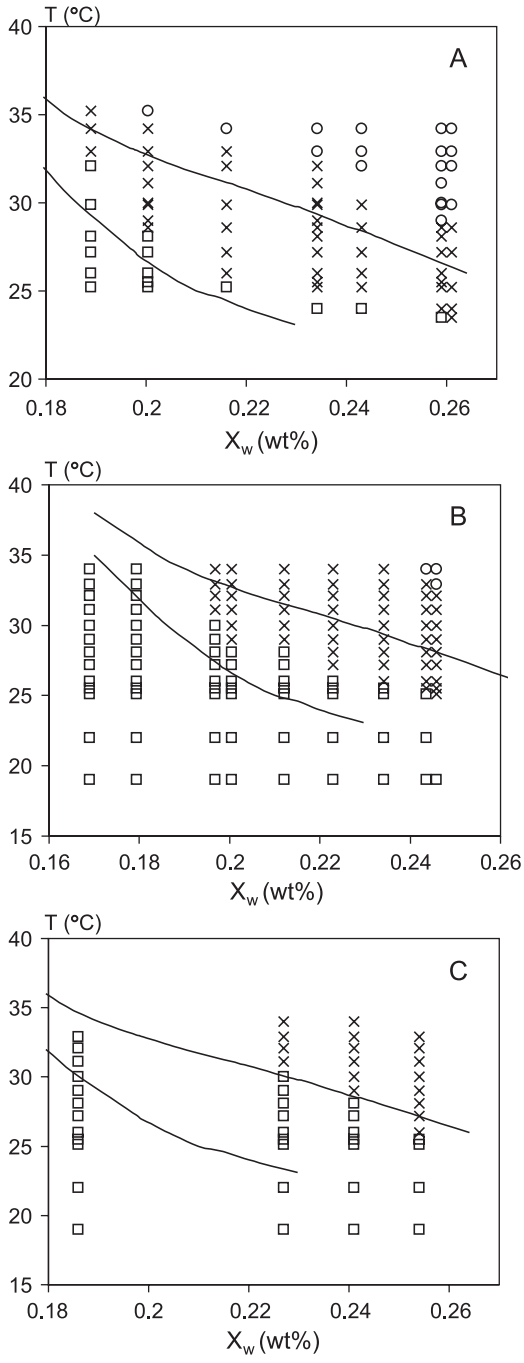

Fig. 3. Partial phase diagrams for the (A) MO–OG–water, (B) MO–bR–water and (C) MO–OG–bR–water systems. The samples were characterized as lamellar phase (□), cubic phase (○) or as coexisting lamellar and cubic phases (×). The ternary and quaternary samples were prepared so that the ratio of OG/MO and bR/MO were kept constant to 1 and 0.5 wt.%, respectively, and the water content is expressed as $X_w=m_w/m_{tot}$, where m_w is the amount of water and m_{tot} is the total mass of the sample. For comparison, the phase boundaries obtained for the binary MO–water system are also included in the figures (solid lines). The phase characterization was performed by visual inspection and SAXS measurement, and anisotropy was detected in plane polarized light. It is shown that both bR and OG stabilize the lamellar phase in favor of the cubic phase.

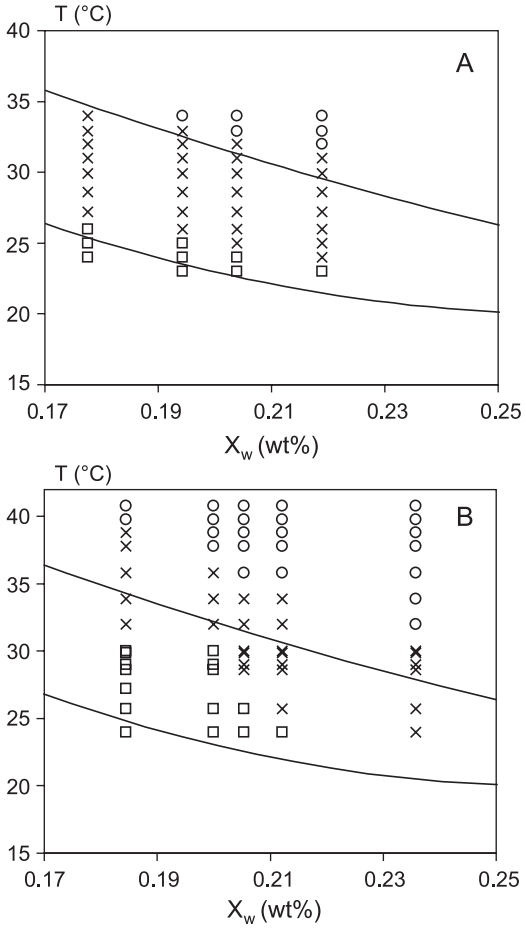

Fig. 4. Partial phase diagrams for the (A) MO–DSPG–OG–water and (B) MO–DSPG–bR–water. The samples were characterized as lamellar phase (□), cubic phase (○) or as coexisting lamellar and cubic phases (×). The samples were prepared so that the ratio of OG/(MO+DSPG) and bR/(MO+DSPG) were kept constant to 1 and 0.5 wt.%, respectively, and the weight ratio MO/DSPG was 22.4:1. For comparison, the phase boundaries obtained for the ternary MO–DSPG–water system are also included in the figures (solid lines). The phase characterization was performed by visual inspection and SAXS measurement, and anisotropy was detected in plane polarized light. It is shown that both bR and OG stabilize the lamellar phase in favor of the cubic phase.

In the fully hydrated systems, the cubic phase is present also in the presence of a small amount of OG. This has also been demonstrated for a large range of different detergents that are suitable for protein crystallization [26]. When the amount of OG is increased, the lamellar phase is expected to be present at even higher water contents. In fact, small angle X-ray diffraction studies of a mixture of MO–OG have shown that, at an OG level of 38 wt.%, the lamellar phase is stable in excess water [27,28]. In like manner, the OG homologue, dodecyl maltoside (DM), has been shown to destabilize the cubic phase in favor of the lamellar structure [29]. It has also been shown that OG promotes the lamellar phase over the bicontinuous 'molten cubic' L_3 (sponge) phase in a ternary system of MO, water and *N*-methyl-α-pyrrolidone (NMP) [30].

To explain the effects caused by the incorporation of transmembrane proteins, such as bR, in the lipid bilayers (Figs. 3B,C and 4B), it is appropriate to use the concept of hydrophobic mismatch. When a protein is incorporated in the lipid bilayer, mismatch between the length and the shape of the hydrophobic part of the membrane-spanning protein and the hydrophobic region of the lipid bilayer will occur [31]. The hydrophobic thickness of bR has been estimated to 31 Å [32], which is comparable of the thickness of the MO bilayer (35 Å) [10]. However, the hydrophobic part of a transmembrane protein can be depicted as a rigid cylinder with a diameter much larger than the diameter of the hydrocarbon chain of MO [10].

It is likely that the insertion of a membrane protein puts geometrical constraints on the lipid packing, and one can expect a more favorable hydrophobic match to the bilayer of zero curvature in the lamellar phase, than to the saddle-shaped (highly curved) bilayer of the cubic phase. One consequence of the curvature-related mismatch can be that the lamellar phase is more readily induced in the presence of the transmembrane protein, and that the proteins are accumulated in domains of lamellar phase within the cubic phase [10]. This model is supported by the results in Figs. 3A and 4B, showing that the lamellar phase is induced at higher water contents when bR is incorporated in the bilayer. It has also been treated in a theoretical analysis by Grabe et al. [33], showing that the lamellar phase was stabilized when the proteins, embedded in the cubic phase, cluster together in flattened regions of the membrane.

When interpreting the data in Figs. 3B,C and 4B, we notice the possibility that a small amount of lipids from the native membrane still may be present (less than 0.1 mol% [10]), even though the protein is purified. The purple membrane lipid classes are phosphatidyl glycerophosphate (PGP-Me), phosphatidyl glycerol (PG), phosphatidyl glycerosulfate (PGPS) and squalene [34], which can promote the formation of a lamellar phase in the same manner as OG. Thus, the observed stabilization of the lamellar phase by bR might partly be attributed to the presence of membrane lipids.

3.4. bR crystallization in the MO–DSPG–water system

It is plausible that the applicability of the in cubo method for crystallization of membrane proteins is dependent on the internal dimensions of the cubic phase and the lamellar phase. It is therefore desirable to regulate the geometrical properties of the lipid phase and, at the same time, retain the properties of a bicontinuous cubic phase in excess water and a transition to a lamellar phase at lower water contents. The addition of detergent that promotes the formation of the lamellar phase could slightly affect the dimensions of the lamellar phase at the phase transition. In order to alter the dimensions in a more pronounced way, the chemical composition of the lipid phase can be modified. One approach to modify the

lipid composition, so that geometrical restrictions of the phase are adjusted, is to add a charged lipid, e.g., DSPG to the MO cubic phase.

Crystals were grown from the binary MO-cubic phase (C_D) and from the ternary MO–DSPG cubic phases (C_G and C_P) (Table 3, Fig. 5). The crystals grown in the MO–DSPG cubic phase appeared more often than those grown in the MO cubic phase and the crystals appeared equally often when grown from the different MO–DSPG cubic phases. Furthermore, the crystals appeared slightly larger and grew a little faster in the MO–DSPG cubic phases. A comparison was, however, not made between the different crystals, so no conclusions can be drawn on quality differences.

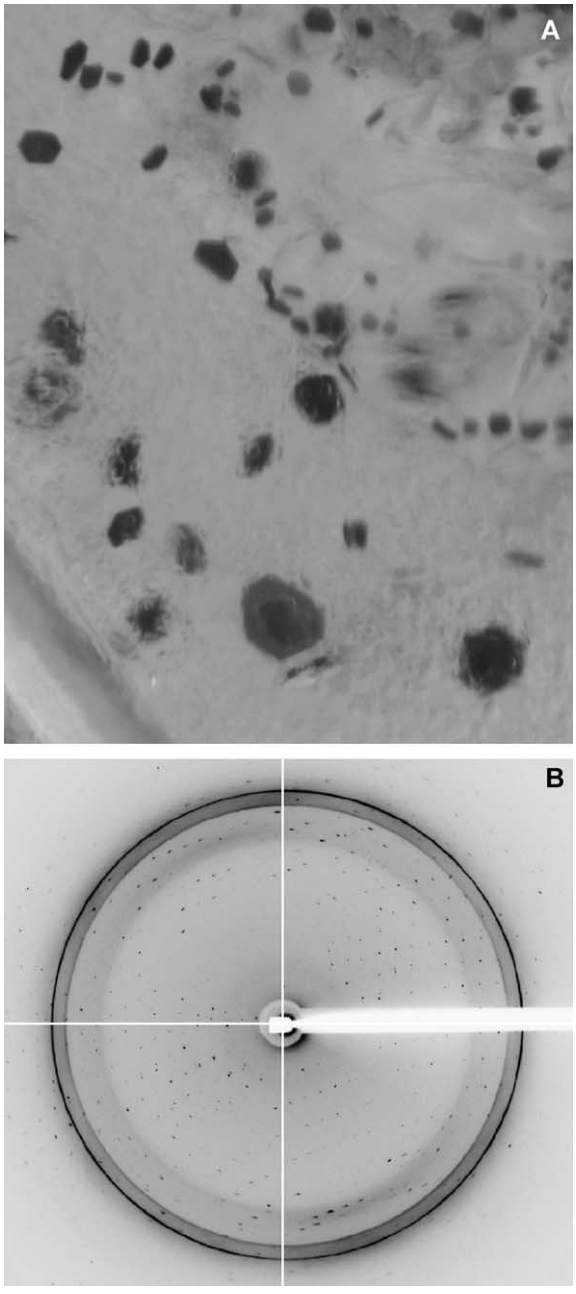

Fig. 5. bR crystals grown from a cubic phase of MO, DSPG and buffer solution with the corresponding diffraction pattern. (A) The crystals grew as hexagonal plates around 70 μm across and between 5- and 10-μm thick. (B) Crystal diffracting to 2.8 Å at 100 K.

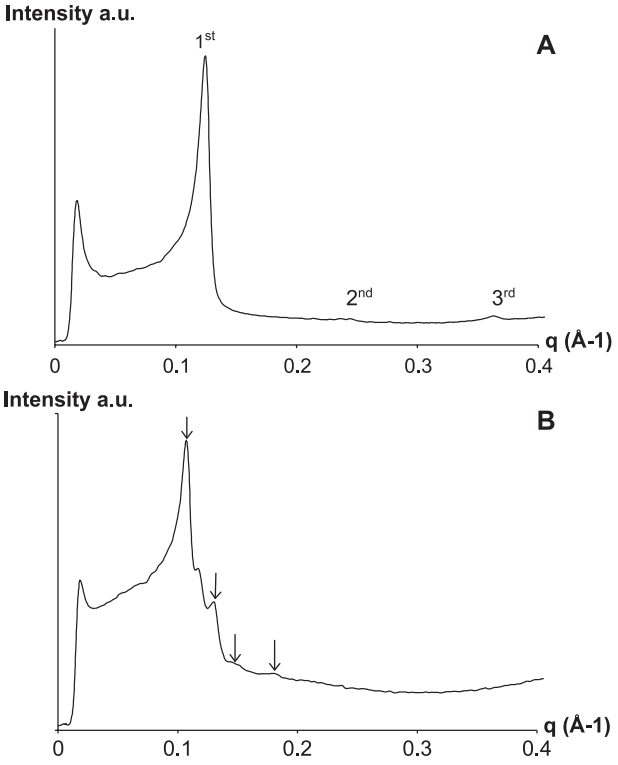

Fig. 6. SAXS diffraction patterns for a sample of MO–DSPG buffer with bR crystals. (A) 20 °C. The arrows indicate the first, second and third order of diffraction peaks from a lamellar phase (lattice spacing of 50.4 Å). (B) 25 °C. The arrows indicate four diffraction peaks that are consistent with a cubic phase (*Pn*3*m*, lattice spacing of 83.5 Å). The diffraction peak at q=0.117 $Å^{-1}$ does not fit with the *Pn*3*m* space group. This peak may reflect a lamellar phase (lattice spacing 53.8 Å).

SAXS studies were undertaken on the MO–DSPG system after the formation of bR crystals at 20 and 25 °C, respectively (see Fig. 6). The SAXS data at 20 °C reveal a lamellar phase with a lattice spacing of 50.4 Å. At 25 °C, a more complicated diffraction pattern appears, which shows the best match with a cubic phase (*Pn*3*m*, lattice spacing 83.5 Å) for four of the diffraction peaks according to the indexing given in Fig. 6B. The diffraction peak at q=0.117 $Å^{-1}$, which does not fit with the *Pn*3*m* space group, may reflect a lamellar phase (lattice spacing 53.8 Å). In the work by Engblom et al. [11] on the MO–DSPG–water system, the lamellar phase can only be in equilibrium with a C_G cubic phase, and therefore, their findings do not support our interpretation. However, the occurrence of bR, OG and Sørensen salt in our system makes a direct comparison difficult. Vargas et al. [35] found that adding Sorensen salt (i.e., sodium and potassium phosphate) in the range 0.5 to 2.0 M to the MO–water system at neutral pH resulted in C_D cubic phases with spacings in the range 99.5 to 77.2 Å.

Furthermore, the data in Fig. 6 demonstrate that dehydrated samples are very close to the phase boundary between the cubic and the lamellar phases, indicating that the sample is very close to the phase transition, and that the presence of the lamellar phase is compatible with the conditions required for crystal growth. These results are consistent with previous reports on microscopic inspection of crystal-containing samples in plane polarized light, stating that the bR crystals appeared enveloped by a layer of blue birefringence, indicative of a anisotropic lipid lamellar phase, whereas the bulk phase was non-birefringent [10,36].

4. Conclusion

The underlying mechanism for in cubo crystallization is still not fully understood. In this work, we propose that the anomalous phase behavior of MO and water upon dehydration and the phase transition to a lamellar phase are crucial for in cubo crystallization of membrane proteins. It has been suggested that the lamellar phase may be induced by the presence of membrane proteins due to a more favorable hydrophobic match [10], which is also supported by the results of the present study showing that bR has a stabilizing effect on the lamellar phase. We also demonstrate that the samples in which protein crystals grow are close to the lamellar phase. The fact that the transition enthalpy is very low and that the transition occurs at a high water activity implies that the lamellar phase is formed rather readily when the system is dehydrated. In the dehydrated sample, the proteins can accumulate in domains of lamellar phase, where nucleation and crystal growth can take place. The dehydration of the cubic phase can therefore be regarded as a 'chasing' of the membrane proteins into small domains where the crystals can grow. In the presence of salt, one can also expect short-range electrostatic screening effects, which could allow the proteins to pack closer. This mechanism may be important in the final state of the crystallization process when the proteins are already accumulated in small domains.

We further suggest that the internal dimensions of the lipid liquid crystalline phases play an important role for in cubo crystallization. Numerous studies have been reported on experimental protocols for the crystallization, exploring different lipid phases, detergents, screen solutions, etc. Table 3 summarizes some aspects of different crystallization protocols in the present study. These data can be correlated to the phase behavior of the corresponding lipid systems. In the present study, we demonstrate that crystals of bR can be grown from both the C_P and the C_G cubic phases of MO–DSPG. It does not appear that the space group of the cubic phase has an impact on the crystallization, but rather on the water content and the dehydration treatment.

Table 3
Crystallization conditions for bR

Initial phase	Detergent	Salt	Successful setups	Comments
MO (C_D)	OG	Na/K phosphate	36% (4/11)	
MO (C_D)	–	Na/K phosphate	50% (1/2)	small crystals
MO–DSPG (C_P)	OG	Na/K phosphate	75% (3/4)	
MO–DSPG (C_P)	–	Na/K phosphate	75% (3/4)	small crystals
MO–DSPG (C_G)	OG	Na/K phosphate	75% (3/4)	
MO–DSPG (C_G)	–	Na/K phosphate	50% (2/4)	small crystals

Crystallization appeared to occur more readily in the presence of DSPG and OG. It is possible that the alteration in phase behavior relieves some geometrical constrains set by the dimensions of the lipid phase, which might facilitate protein accumulation and crystal growth. The addition of a small amount detergent/anionic lipid was shown to induce the lamellar phase at higher water content compared to the MO–water system. This implies a more swollen lamellar phase, which might facilitate crystal growth. It was also observed that the crystals grown in the absence of detergent and/or anionic lipids are smaller than those grown in the presence of these additives. These findings are expectedly important for the design of new systems for in cubo crystallization of membrane proteins.

Acknowledgements

We thank Annika Ridell for help with the X-ray measurements. The opportunity for PW to work with Karl Edman, Gergely Katona, Richard Neutze and Arjan Snijder at the Department of Molecular Biotechnology, Chalmers is gratefully acknowledged.

Appendix A. Calculation of the transition enthalpy and the transition entropy

The calorimetric data can be utilized to calculate values of the transition enthalpy, $\Delta H^{L_\alpha \rightarrow C_G}$, and the transition entropy, $\Delta S^{L_\alpha \rightarrow C_G}$. $\Delta H^{L_\alpha \rightarrow C_G}$ is obtained from integrating the enthalpy curve over the phase transition, and $\Delta S^{L_\alpha \rightarrow C_G}$ is then directly calculated as

$$\Delta S^{L_\alpha C_G} = \frac{\Delta H^{L_\alpha \rightarrow C_G}}{T} \quad \text{(A1)}$$

If $\Delta H^{L_\alpha \rightarrow C_G}$ cannot be obtained from the calorimetric data, it is still possible to make a thermodynamic analysis of the phase transition using van der Waals differential

equation [19,37], based on the temperature dependence in the activity curves (Fig. 1A)

$$\left(\frac{dT}{dx}\right)^{L_\alpha} = -\frac{RT\left(\frac{d\ln a_w}{(1-x)dx}\right)_{T,P}^{(L_\alpha)}\Delta x^{L_\alpha\rightarrow C_G}}{S^{m(C_G)} - S^{m(L_\alpha)} - \Delta x^{L_\alpha\rightarrow C_G}\left(\partial S^m/\partial x\right)_{T,P}^{(L_\alpha)}} = -\frac{RT\left(\frac{d\ln a_w}{(1-x)dx}\right)_{T,P}^{(L_\alpha)}\Delta x^{L_\alpha\rightarrow C_G}}{\Delta S^{L_\alpha\rightarrow C_G}} \quad (A2)$$

where x is the mole fraction of water. The slope of the phase boundary $(dT/dx)^{(1)}$ can be calculated from the composition of the lamellar phase at different temperatures (Table 1). The water uptake ($\Delta x^{L_\alpha\rightarrow C_G}$) and the derivative of the activity can be obtained from activity curves (Fig. 1A).

Appendix B. Interaction forces calculated from the calorimetric sorption data

The calorimetric sorption measurement provides a relation between water content and the osmotic pressure of water, Π_{osm}

$$\Delta\mu_w = -V_w\Pi_{osm} = RT\ln(a_w) \quad (A3)$$

In the lamellar systems of uncharged lipids, this is often recast as a force–distance relation and it has been called the hydration force. The hydration force is generally considered as exponentially decaying with the interlamellar distance [38]. If the lamellar system is considered as incompressible, one can also expect an exponential decay of the osmotic pressure with respect to the water content.

$$\Pi_{osm} = F/\text{area} = F_0 e^{-(n_w/n_{MO})/\lambda} \quad (A4)$$

where F_0 is the amplitude of the repulsive force and λ is the decay length with respect to the number of water molecules per lipid (n_w/n_{MO}).

The curvature elastic free energy of a cubic phase can be written in terms of the mean $\langle H\rangle$ and the Gaussian $\langle K\rangle$ curvature at the neutral surface of the lipid monolayer as

$$\Delta G_c = 2k_c\left(\langle H^2\rangle - 2H_0\langle H\rangle + 2H_0^2\right) + k_g\langle K\rangle \quad (A5)$$

where k_c is the rigidity bending constant, k_g is the Gaussian curvature constant, H_0 is the spontaneous curvature, and $\langle H^2\rangle$ represents the second moment of the mean curvature [39]. The averages of all these parameters are dependent on the lattice parameter, a, and are obtained from established relationships [39,40]. Finally, the lattice parameter, a, is related to the water content, X_w, and the bilayer thickness, l, as

$$X_w = 1 - 2\sigma\frac{1}{a} - \frac{4}{3}\pi\chi\left(\frac{l}{a}\right)^3 \quad (A6)$$

where σ and χ are the minimal surface constants. For the C_G bicontinuous cubic phases, σ=3.091 and χ=−8 [41]. When combining Eqs. A5 and A6, the numerical relation between the curvature elastic free energy and the water/lipid ratio can be obtained. Data for the variation in l were obtained from Ref. [42]. The theoretical relationship can be compared to the experimental data for the free energy, by integration of the chemical potential of water, $\Delta\mu_w$, with respect to the number of mole water. $\Delta\mu_w$ is directly related to the water activity, a_w, according to Eq. (A3). For these calculations, the experimental data were extrapolated to the limit of full hydration ($\Delta\mu_w$=0).

References

[1] E.M. Landau, J.P. Rosenbusch, Lipidic cubic phases: A novel concept for the crystallization of membrane proteins, Proc. Natl. Acad. Sci. U. S. A. 93 (1996) 14532–14535.

[2] M.L. Chiu, P. Nollert, M.C. Loewen, H. Belrhali, E. Pebay-Peyroula, J.P. Rosenbusch, E.M. Landau, Crystallization in cubo: general applicability to membrane proteins, Acta Crystallogr., D 56 (Pt. 6) (2000) 781–784.

[3] M. Kolbe, H. Besir, L.O. Essen, D. Oesterhelt, Structure of the light-driven chloride pump halorhodopsin at 1.8 Å resolution, Science 288 (2000) 1390–1396.

[4] H. Luecke, B. Schobert, J.K. Lanyi, E.N. Spudich, J.L. Spudich, Crystal Structure of Sensory Rhodopsin II at 2.4 angstroms: insights into color tuning and transducer interaction, Science 293 (2001) 1499–1503.

[5] V.I. Gordeliy, J. Labahn, R. Moukhametzianov, R. Efremov, J. Granzin, R. Schlesinger, G. Bueldt, T. Savopol, A.J. Scheidig, J.P. Klare, M. Engelhard, Molecular basis of transmembrane signalling by sensory rhodopsin II–transducer complex, Nature 419 (2002) 484–487.

[6] G. Katona, U. Andreasson, E.M. Landau, L.E. Andreasson, R. Neutze, Lipidic cubic phase crystal structure of the photosynthetic reaction centre from Rhodobacter sphaeroides at 2.35 Å resolution, J. Mol. Biol. 331 (2003) 681–692.

[7] J. Briggs, H. Chung, M. Caffrey, The temperature–composition phase diagram and mesophase structure characterization of the monoolein/water system, J. Phys., II 6 (1996) 723–751.

[8] S. Hyde, S. Andersson, B. Ericsson, K. Larsson, A cubic structure consisting of a lipid bilayer forming an infinite periodic minimum surface of the gyroid type in the glycerolmonooleate–water system, Z. Kristallogr. 168 (1984) 213–219.

[9] B. Jönsson, B. Lindman, K. Holmberg, B. Kronberg, Surfactants and Polymers in Aqueous Solution, John Wiley & Son, Chichester, 1998.

[10] P. Nollert, H. Qiu, M. Caffrey, J.P. Rosenbusch, E.M. Landau, Molecular mechanism for the crystallization of bacteriorhodopsin in lipidic cubic phases, FEBS Lett. 504 (2001) 179–186.

[11] J. Engblom, Y. Miezis, T. Nylander, V. Razumas, K. Larsson, On the swelling of monoolein liquid-crystalline aqueous phases in the presence of distearoylphosphatidylglycerol, Prog. Colloid Polym. Sci. 116 (2000) 9–15.

[12] A. Kristensen, T. Nylander, M. Paulsson, A. Carlsson, Calorimetric studies of interactions between beta-lactoglobulin and phospholipids in solutions, Int. Dairy J. 7 (1997) 87–92.

[13] T. Landh, Cubic phases and cubosomes in lipid–water systems, Licentiate thesis, Lund University, Lund, 1991.

[14] I. Wadsö, L. Wadsö, A second generation twin double micro-calorimeter—Measurements of sorption isotherms, heats of sorption and sorption kinetics, J. Therm. Anal. 49 (1997) 1045–1052.

[15] L. Wadsö, N. Markova, A method to simultaneously determine sorption isotherms and sorption enthalpies with a double twin microcalorimeter, Rev. Sci. Instrum. 73 (2002) 2743–2754.
[16] L. Wadsö, N. Markova, A double twin isothermal microcalorimeter, Thermochim. Acta 360 (2000) 101–107.
[17] V. Kocherbitov, L. Wadsö, A desorption calorimetric method for use at high water activities, Thermochim. Acta 411 (2004) 31–36.
[18] G.H. Rummel, A. Hardmeyer, C. Widmer, M.L. Chiu, P. Nollert, K.P. Locher, E.M. Landau, J.P. Rosenbusch, Lipidic cubic phases: new matrices for the three-dimensional crystallization of membrane proteins, J. Struct. Biol. 121 (1998) 82–91.
[19] V. Kocherbitov, O. Söderman, L. Wadsö, Phase diagram and thermodynamics of the *n*-octyl beta-D-glucoside/water system, J. Phys. Chem., B 106 (2002) 2910–2917.
[20] H. Chung, M. Caffrey, The curvature elastic-energy function of the lipid–water cubic mesophase, Nature 368 (1994) 224–226.
[21] M. Vacklin, B.J. Khoo, K.H. Madan, J.M. Seddon, R.H. Templer, The bending elasticity of 1-monoolein upon relief of packing stress, Langmuir 16 (2000) 4741–4748.
[22] R.P. Rand, Interacting phospholipid bilayers: measured force and induced structural changes, Annu. Rev. Biophys. Bioeng. 10 (1981) 277–314.
[23] S. Engström, L. Lindahl, R. Wallin, J. Engblom, A study of polar lipid drug systems undergoing a thermoreversible lamellar-to-cubic phase transition, Int. J. Pharm. 86 (1992) 137–145.
[24] H. Qiu, M. Caffrey, The phase diagram of the monoolein/water system: metastability and equilibrium aspects, Biomaterials 21 (2000) 223–234.
[25] J.N. Israelachvili, S. Marcelja, R. Horn, Physical principles of membrane organization, Q. Rev. Biophys. 13 (1980) 121–200.
[26] C. Sennoga, A. Heron, J.M. Seddon, R.H. Templer, B. Hankamer, Membrane-protein crystallization in cubo: temperature-dependent phase behaviour of monoolein–detergent mixtures, Acta Crystallogr., D 59 (2003) 239–246.
[27] B. Angelov, M. Ollivon, A. Angelova, X-ray diffraction study of the effect of the detergent octyl glucoside on the structure of lamellar and nonlamellar lipid/water phases of use for membrane protein reconstitution, Langmuir 15 (1999) 8225–8234.
[28] G. Persson, H. Edlund, G. Lindblom, Thermal behaviour of cubic phases rich in 1-monooleoyl-rac-glycerol in the ternary system—1-monooleoyl-rac-glycerol/*n*-octyl-beta-D-glucoside/water, Eur. J. Biochem. 270 (2003) 56–65.
[29] X. Ai, M. Caffrey, Membrane protein crystallization in lipidic mesophases: Detergent effects, Biophys. J. 79 (2000) 394–405.
[30] K. Ekelund, Lipid bilayers versus monolayers. Sponge phases and skin lipid domains, Doctorial thesis, Lund University, Lund, 2000.
[31] J.A. Killian, Hydrophobic mismatch between proteins and lipids in membranes, Biochim. Biophys. Acta 1376 (1998) 401–416.
[32] B. Piknova, E. Perochon, J.F. Tocanne, Hydrophobic mismatch and long-range protein–lipid interactions in bacteriorhodopsin phosphatidylcholine vesicles, Eur. J. Biochem. 218 (1993) 385–396.
[33] M. Grabe, J. Neu, G. Oster, P. Nollert, Protein interactions and membrane geometry, Biophys. J. 84 (2003) 854–868.
[34] S. Dracheva, S. Bose, R.W. Hendler, Chemical and functional studies on the importance of purple membrane lipids in bacteriorhodopsin photocycle behavior, FEBS Lett. 382 (1996) 209–212.
[35] R. Vargas, L. Mateu, A. Romero, The effect of increasing concentrations of precipitating salts used to crystallize proteins on the structure of the lipidic Q224 cubic phase, Chem. Phys. Lipids 127 (2004) 103–111.
[36] M. Caffrey, A lipid's eye view of membrane protein crystallization in mesophases, Curr. Opin. Struck. Biol. 10 (2000) 486–497.
[37] A.M. Toikka, J.D. Jenkins, Conditions of thermodynamic equilibrium and stability as a basis for the practical calculation of vapour–liquid equilibria, Chem. Eng. J. 89 (2002) 1–27.
[38] L.J. Lis, M. McAlister, N. Fuller, R.P. Rand, V.A. Parsegian, Interactions between neutral phospholipid bilayer membranes, Biophys. J. 37 (1982) 657–666.
[39] D.M. Anderson, S.M. Gruner, S. Leibler, Geometrical aspects of the frustration in the cubic phases of lyotropic liquid-crystals, Proc. Natl. Acad. Sci. U. S. A. 85 (1988) 5364–5368.
[40] D.C. Turner, Z.G. Wang, S.M. Gruner, D.A. Mannock, R.N. McElhaney, Structural study of the inverted cubic phases of di-dodecyl alkyl-beta-D-glucopyranosyl-rac-glycerol, J. Phys., II 2 (1992) 2039–2063.
[41] S. Andersson, S.T. Hyde, K. Larsson, S. Lidin, Minimal surfaces and structures: from inorganic and metal crystals to cell membranes and biopolymers, Chem. Rev. 88 (1988) 221–242.
[42] M. Pisani, S. Bernstorff, C. Ferrero, P. Mariani, Pressure induced cubic-to-cubic phase transition in monoolein hydrated system, J. Phys. Chem., B 105 (2001) 3109–3119.